ORGANOMETALLICS

Volume 18, Number 4, February 15, 1999

Articles

Nature of the Metal−Alkene Bond in Platinum Complexes of Strained Olefins

Jamal Uddin, Stefan Dapprich, and Gernot Frenking*

Fachbereich Chemie, Philipps-Universität Marburg, Hans-Meerwein-Strasse, D-35032 Marburg, Germany

Brian F. Yates*

School of Chemistry, University of Tasmania, GPO Box 252C, Hobart TAS 7001, Australia

Received July 9, 1998

Density functional theory and high-level *ab initio* molecular orbital methods have been used to investigate complexes of platinum with highly pyramidalized olefins: $Pt(PH_3)_2(R)$ with R = $C_{11}H_{16}$, $C_{10}H_{14}$, C_9H_{12}, and C_8H_{10}. Geometries and binding energies are reported and compared to experimental values where available. Charge decomposition analyses have been carried out for all complexes, and they show a beautiful increase in olefin←Pt back-donation as the olefin becomes more pyramidal. Natural bond orbital analyses show a corresponding increase in the platinum 6s and carbon 2s character in the Pt−C bond orbital, in agreement with previous NMR studies. We also find that the binding energies of all the complexes correlate well with the olefin strain energies calculated for the free olefins.

Introduction

Platinum−olefin complexes have been studied in detail over a number of years, with the incorporation of a wide range of olefins and associated ligands.[1−3] One of the most interesting aspects of these compounds is the ability of PtL_2 (L = PPh_3, for example) to stabilize strained olefins upon formation of the complex. This has been exploited particularly by Borden and co-workers,[4,5] and the approach has also been used to stabilize cyclopropenes[6−9] and cycloalkynes.[10−12]

* To whom correspondence should be addressed. Fax: +61 3 6226-2858. E-mail: Brian.Yates@utas.edu.au.

(1) Ittel, S. D.; Ibers, J. A. *Adv. Organomet. Chem.* **1976**, *14*, 33−61.
(2) Hartley, F. R. In *Comprehensive Organometallic Chemistry*; Wilkinson, G., Ed.; Pergamon: London, 1982; Vol. 6, pp 471−762.
(3) Young, G. B. In *Comprehensive Organometallic Chemistry II*; Abel, E. W., Stone, F. G. A., Wilkinson, G., Eds.; Pergamon: London, 1995; Vol. 9, pp 533−587.
(4) Kumar, A.; Lichtenhan, J. D.; Critchlow, S. C.; Eichinger, B. E.; Borden, W. T. *J. Am. Chem. Soc.* **1990**, *112*, 5633−5634.
(5) Nicolaides, A.; Smith, J. M.; Kumar, A.; Barnhart, D. M.; Borden, W. T. *Organometallics* **1995**, *14*, 3475−3485.
(6) Visser, J. P.; Schipperijn, A. J.; Lukas, J. *J. Organomet. Chem.* **1973**, *47*, 433−438.
(7) de Boer, J. J.; Bright, D. *J. Chem. Soc., Dalton Trans.* **1975**, 662−665.
(8) Leigh, G. J.; McMahon, C. N. *J. Organomet. Chem.* **1995**, *500*, 219−225.
(9) Hughes, D. L.; Leigh, G. J.; McMahon, C. N. *J. Chem. Soc., Dalton Trans.* **1997**, 1301−1307.

10.1021/om9805842 CCC: $18.00
Publication on Web 01/20/1999

The simplest olefin complex of this type, $Pt(PPh_3)_2(C_2H_4)$,[13,14] has been modeled by sophisticated molecular orbital calculations on **1.**[15] In that work, Morokuma and

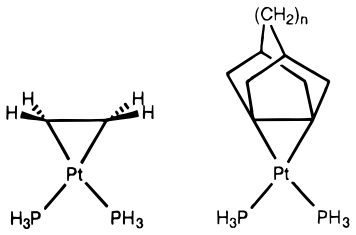

1

2 n=3
3 n=2
4 n=1
5 n=0

Borden discussed the nature of the donor−acceptor binding in **1** and showed that increasing the pyramidalization angle (defined as the angle ϕ between the C−C bond and the plane containing CH_2) corresponds to an increase in the olefin←Pt back-donation as calculated from Mulliken population analyses. The standard model of bonding in metal−olefin complexes of this type is that due to Dewar, Chatt, and Duncanson[16,17] and has been confirmed by molecular orbital calculations.[18] The nature of the bonding in **1** has been studied many times by computational chemists.[15,19−31] Indeed, nearly 20 years ago Ziegler and Rauk[23] performed a careful energy decomposition study on (unoptimized) structures in order to elucidate the relative importance of olefin→Pt donation and olefin←Pt back-donation effects in different conformers. They showed that back-donation is more important for the stability of the complex. This does not mean that there is more olefin←metal back-donation than olefin→metal donation. Because of the better overlap, donation should be larger than back-donation. The dominant σ-type donation of the olefin is offset, however, by repulsive interactions with occupied σ(d) orbitals of the metal.[23] A number of recent computational papers have also studied **1** from the point of view of comparing the bonding with that in Pt−C_{60} complexes.[28,29,31] In a detailed study,[31] Bader charges and critical points for **1** were evaluated and these showed the expected changes in electron density arising from donor−acceptor bonding.

Recently, Borden[4,5] has described the first syntheses and X-ray structures of $Pt(PPh_3)_2$ complexes of a series of highly pyramidalized tricyclic alkenes, shown by structures **2**−**4** (with PPh_3 instead of PH_3). The last member of this series, the remarkable complex with $n = 0$ (**5**), has not yet been synthesized, but the bis(ethano)[32] and dimethyl[33] analogues of the uncomplexed tricyclic alkene with $n = 0$ have themselves been made recently. Pyramidalized alkenes have been the subject of a number of reviews.[34,35]

In this paper we report our studies of complexes **1**−**5** with high-level theoretical methods. Our aim is to analyze the nature of the bonding interactions in these complexes and to predict theoretically Pt−olefin binding energies. To this end we have used our charge decomposition analysis procedure,[36] which we have shown previously to provide useful information about the metal−ligand bonding in transition-metal complexes.[18] The binding energies are calculated at the CCSD(T) level using our standard basis set II, which gives highly accurate bond energies for transition-metal complexes.[20,37−45]

Theoretical Methods

Full geometry optimizations for systems **1**−**5** and the corresponding fragments $Pt(PH_3)_2$, ethene, and the four tricyclic alkenes with $n = 0$, 1, 2, and 3 were carried out with the use of the B3LYP[46,47] density functional level of theory and our standard "Basis Set II",[20] which incorporates the Hay and Wadt[48] small-core relativistic effective core potential and

(10) Bennett, M. A.; Yoshida, T. *J. Am. Chem. Soc.* **1978**, *100*, 1750.
(11) Bennett, M. A. *Pure Appl. Chem.* **1989**, *61*, 1695.
(12) Bennett, M. A.; Schwemlein, H. P. *Angew. Chem., Int. Ed. Engl.* **1989**, *28*, 1296.
(13) Cheng, P.-T.; Cook, C. D.; Nyburg, S. C.; Wan, K. Y. *Inorg. Chem.* **1971**, *10*, 2210−2213.
(14) Cheng, P.-T.; Nyburg, S. C. *Can. J. Chem.* **1972**, *50*, 912−916.
(15) Morokuma, K.; Borden, W. T. *J. Am. Chem. Soc.* **1991**, *113*, 1912−1914.
(16) Dewar, M. J. S. *Bull. Soc. Chim. Fr.* **1951**, *18*, C71−C79.
(17) Chatt, J.; Duncanson, L. A. *J. Chem. Soc.* **1953**, 2939−2947.
(18) Frenking, G.; Pidun, U. *J. Chem. Soc., Dalton Trans.* **1997**, 1653−1662.
(19) Rösch, N.; Messner, R. P.; Johnson, K. H. *J. Am. Chem. Soc.* **1974**, *96*, 3855−3860.
(20) Frenking, G.; Antes, I.; Böhme, M.; Dapprich, S.; Ehlers, A. W.; Jonas, V.; Neuhaus, A.; Otto, M.; Stegmann, R.; Veldkamp, A.; Vyboishchikov, S. F. In *Reviews in Computational Chemistry*; Lipkowitz, K. B., Boyd, D. B., Eds.; VCH: New York, 1996; Vol. 8, pp 63−144.
(21) Norman, J. G. *Inorg. Chem.* **1977**, *16*, 1328−1335.
(22) Mingos, D. M. P. *Adv. Organomet. Chem.* **1977**, *15*, 1−51.
(23) Ziegler, T.; Rauk, A. *Inorg. Chem.* **1979**, *18*, 1558−1565.
(24) Albright, T. A.; Hoffmann, R.; Thibeault, J. C.; Thorn, D. L. *J. Am. Chem. Soc.* **1979**, *101*, 3801−3812.
(25) Ziegler, T. *Inorg. Chem.* **1985**, *24*, 1547−1552.
(26) Ziegler, T. *J. Chem. Soc. Chem. Commun.* **1989**, 86−88.
(27) Sakaki, S.; Ieki, M. *Inorg. Chem.* **1991**, *30*, 4218−4224.
(28) Koga, N.; Morokuma, K. *Chem. Phys. Lett.* **1993**, *202*, 330−334.
(29) Fujimoto, H.; Nakao, Y.; Fukui, K. *J. Mol. Struct.* **1993**, *300*, 425−434.
(30) Li, J.; Schreckenbach, G.; Ziegler, T. *Inorg. Chem.* **1995**, *34*, 3245−3252.
(31) Bo, C.; Costas, M.; Poblet, J. M. *J. Phys. Chem.* **1995**, *99*, 5914−5921.
(32) Branan, B. M.; Paquette, L. A.; Hrovat, D. A.; Borden, W. T. *J. Am. Chem. Soc.* **1992**, *114*, 774−776.
(33) Camps, P.; Font-Bardia, M.; Pérez, F.; Solans, X.; Vázquez, S. *Angew. Chem.* **1995**, *107*, 1011−1013; *Angew. Chem., Int. Ed. Engl.* **1995**, *34*, 912−914.
(34) Hrovat, D. A.; Borden, W. T. *J. Am. Chem. Soc.* **1988**, *110*, 4710−4718.
(35) Borden, W. T. *Chem. Rev.* **1989**, *89*, 1095−1109.
(36) Dapprich, S.; Frenking, G. *J. Phys. Chem.* **1995**, *99*, 9352−9362.
(37) Dapprich, S.; Frenking, G. *Angew. Chem.* **1995**, *107*, 383−386; *Angew. Chem., Int. Ed. Engl.* **1995**, *34*, 354−357.
(38) Ehlers, A. W.; Dapprich, S.; Vyboishchikov, S. F.; Frenking, G. *Organometallics* **1996**, *15*, 105−117.
(39) Dapprich, S.; Frenking, G. *Organometallics* **1996**, *15*, 4547−4551.
(40) Pidun, U.; Frenking, G. *J. Organomet. Chem.* **1996**, *525*, 269−278.
(41) Weiss, J.; Stetzkamp, D.; Nuber, B.; Fischer, R. A.; Böhme, C.; Frenking, G. *Angew. Chem.* **1997**, *109*, 95−97; *Angew. Chem., Int. Ed. Engl.* **1997**, *35*, 70−72.
(42) Szilagyi, R. K.; Frenking, G. *Organometallics* **1997**, *16*, 4807−4815.
(43) Lupinetti, A.; Fau, S.; Frenking, G.; Strauss, S. H. *J. Phys. Chem. A* **1997**, *101*, 9551−9559.
(44) Fischer, R. A.; Schulte, M. M.; Weiss, J.; Zsolnai, L.; Jacobi, A.; Huttner, G.; Frenking, G.; Böhme, C.; Vyboishchikov, S. F.; Frenking, G. *J. Am. Chem. Soc.* **1998,** *120*, 1237−1248.
(45) Vyboishchikov, S. F.; Frenking, G. *Chem. Eur. J.*, in press.
(46) Stephens, P. J.; Devlin, J. F.; Chabalowski, C. F.; Frisch, M. J. *J. Phys. Chem.* **1994**, *98*, 11623−11627.
(47) Hertwig, R. H.; Koch, W. *Chem. Phys. Lett.* **1997**, *268*, 345−351.
(48) Hay, P. J.; Wadt, W. R. *J. Chem. Phys.* **1985**, *82*, 299−310.
(49) Hehre, W. J.; Ditchfield, R.; Pople, J. A. *J. Chem. Phys.* **1972**, *56*, 2257−2261.

Table 1. Theoretical and Experimental Geometrical Parameters (Å and deg)[a] and Metal−Olefin Binding Energies (kJ mol^{-1})[b]

molecule	sym	ϕ[c]	C=C	C−C−R[d]	Pt−C	Pt−P	P−Pt−P	D_e (D_0)
				Compounds **1**−**5**				
1, $Pt(PH_3)_2(C_2H_4)$	C_{2v}	24.1	1.427	119.7	2.152	2.317	107.2	99.9 (93.3)
2, $Pt(PH_3)_2(C_{11}H_{16})$	C_1	48.4[e]	1.446	108.8[e]	2.152[e]	2.323[e]	106.5	147.1 (145.1)
3, $Pt(PH_3)_2(C_{10}H_{14})$	C_2	53.9[e]	1.460	107.8[e]	2.135	2.323	106.6	200.3 (196.3)
4, $Pt(PH_3)_2(C_9H_{12})$	C_{2v}	60.2	1.480	106.6	2.118	2.325	106.4	244.7 (240.3)
5, $Pt(PH_3)_2(C_8H_{10})$	C_{2v}	66.6	1.513	105.1	2.098	2.327	105.6	293.5 (289.0)
				Model Complexes				
1a, $Pt(PH_3)_2(C_2H_4)$	C_{2v}	0.0[f]	1.331[f]	121.9[f]	2.287	2.293	112.2	50.1
1b, $Pt(PH_3)_2(C_2H_4)$	C_{2v}	0.0[g]	1.404	121.7	2.250	2.301	109.7	64.3
1c, $Pt(PH_3)_2(C_2H_4)$	C_{2v}	48.3[h]	1.479	108.9[h]	2.118	2.320	106.9	134.7[i]
1d, $Pt(PH_3)_2(C_2H_4)$	C_{2v}	55.1[h]	1.493	107.5[h]	2.104	2.320	106.9	146.8[i]
1e, $Pt(PH_3)_2(C_2H_4)$	C_{2v}	62.3[h]	1.511	105.9[h]	2.088	2.320	106.8	171.1[i]
1f, $Pt(PH_3)_2(C_2H_4)$	C_{2v}	66.6[h]	1.523	105.1[h]	2.075	2.318	106.7	217.6[i]
				Fragments				
C_2H_4 (ethene)	D_{2h}	0.0	1.331	121.9				
$C_{11}H_{16}$ ($n = 3$)	C_s	27.9[e]	1.342	110.9[e]				
$C_{10}H_{14}$ ($n = 2$)	C_2	42.2[e]	1.349	110.1[e]				
C_9H_{12} ($n = 1$)	C_{2v}	53.7	1.362	108.9				
C_8H_{10} ($n = 0$)	C_{2v}	61.9	1.380	107.5				
$Pt(PH_3)_2$	C_{2v}					2.257	180.0	
				Experimental Structures				
$Pt(PPh_3)_2(C_2H_4)$[j]			1.434		2.112	2.268	111.67	152[k]
$Pt(PPh_3)_2(C_{11}H_{16})$[l]		48.3	1.421	108.9	2.121	2.275	108.7	
$Pt(PPh_3)_2(C_{10}H_{14})$[l]		55.1	1.454	107.5	2.096	2.276	104.7	
$Pt(PPh_3)_2(C_9H_{12})$[l]		62.3	1.475	105.9	2.062	2.289	106.8	

[a] Calculated at B3LYP/II unless otherwise noted. [b] D_e calculated at CCSD(T)/II//B3LYP/II. Estimated value for **2**−**5**; see text. The D_0 values in parentheses include the B3LYP/II ZPVE corrections. [c] Pyramidalization angle. [d] R = H in ethene and C in the tricyclic alkenes. [e] Average of the appropriate values in this point group. [f] Frozen at this value, corresponding to the calculated structure of free ethene. [g] Just the pyramidalization angle is frozen in this case. [h] Frozen at this value, corresponding to experimental (in the case of **1c**−**e**) or calculated (in the case of **1f**) structures; see text. [i] This calculation employed a deformed free ethene molecule with the pyramidalization and C−C−H angles frozen to correspond to the calculated structures of the tricyclic alkenes. [j] From refs 13 and 14; average of X-ray structure values. [k] Gas-phase value from refs 65 and 66; error in this value is quoted as ±18 kJ mol^{-1}. [l] From ref 5; average of X-ray structure values.

double-ζ valence basis sets ((441/2111/21) on platinum and 6-31G(d)[49−51] on the other atoms). Sets of five d functions were used in the basis sets throughout these calculations. Additional geometry optimizations with the BP86/II, BLYP/II, and MP2/II levels of theory were carried out for **1**, but no significant differences from the B3LYP/II geometry were observed. In our calculations on **1**−**5** we approximated the phenyl groups on the phosphines in the experimental structures with simple hydrogens. Harmonic vibrational frequencies were determined analytically for the alkenes, and through evaluation of finite displacements of the first derivatives for the compounds containing platinum (analytic second derivatives involving effective core potentials were not available to us). In each case, the optimized geometries were shown to be true minima. CCSD(T)[52] single-point calculations using the same basis set II were carried out on the B3LYP/II geometries of the smaller complexes and fragments in order to obtain reliable estimates of the binding energies. For the larger complexes we have used the isostructural reaction approach[53] to obtain approximate CCSD(T)/II values for the D_e binding energies from the equation

$$D_{M-L}(\text{CCSD(T)}) \approx D_{M-L}(\text{MP2}) + [D_{M-\text{ethene}}(\text{CCSD(T)}) - D_{M-\text{ethene}}(\text{MP2})]$$

The B3LYP/II vibrational frequencies were used unscaled to calculate zero-point vibrational energy corrections. These molecular orbital calculations were performed with the Gaussian 94[54] and Molpro[55] programs.

A charge decomposition analysis (CDA) for each system was carried out with the CDA[36] program. In the CDA method the (canonical, natural, or Kohn−Sham) molecular orbitals of the complex are expressed in terms of the MOs of appropriately chosen fragments. In the present case, the Kohn−Sham orbitals of the complexes are constructed in the CDA calculation as a linear combination of the orbitals of the fragments: e.g. the olefin ligand and the metal fragment. Thus, three single-point calculations are involved for each system: one on the optimized geometry of the complex, and one on each of the fragments frozen at their geometries in the complex. The orbital contributions to the charge distributions are divided into four parts: (i) the mixing of the occupied orbitals of the olefin and the unoccupied MOs of the metal fragment (olefin→Pt donation *d*), (ii) the mixing of the unoccupied orbitals of the olefin and the occupied MOs of the metal fragment (olefin←Pt back-donation *b*), (iii) the mixing of the occupied orbitals of the olefin and the occupied orbitals of the metal fragment (olefin↔Pt repulsive polarization *r*), and (iv) the mixing of the unoccupied orbitals of the olefin and the unoccupied orbitals of the metal fragment (residual term Δ). The residual term Δ should be ∼0 for true donor−acceptor complexes.[18] A more

(50) Francl, M. M.; Pietro, W. J.; Hehre, W. J.; Binkley, J. S.; Gordon, M. S.; DeFrees, D. J.; Pople, J. A. *J. Chem. Phys.* **1982**, *77*, 3654−3665.
(51) Hariharan, P. C.; Pople, J. A. *Chem. Phys. Lett.* **1972**, *16*, 217−219.
(52) Pople, J. A.; Head-Gordon, M.; Raghavachari, K. *J. Chem. Phys.* **1987**, *87*, 5968−5975.
(53) Dapprich, S.; Pidun, U.; Ehlers, A. W.; Frenking, G. *Chem. Phys. Lett.* **1995**, *242*, 521−526.
(54) Frisch, M. J.; Trucks, G. W.; Schlegel, H. B.; Gill, P. M. W.; Johnson, B. G.; Robb, M. A.; Cheeseman, J. R.; Keith, T.; Petersson, G. A.; Montgomery, J. A.; Raghavachari, K.; Al-Laham, M. A.; Zakrzewski, V. G.; Ortiz, J. V.; Foresman, J. B.; Cioslowski, J.; Stefanov, B. B.; Nanayakkara, A.; Challacombe, M.; Peng, C. Y.; Ayala, P. Y.; Chen, W.; Wong, M. W.; Andres, J. L.; Replogle, E. S.; Gomperts, R.; Martin, R. L.; Fox, D. J.; Binkley, J. S.; Defrees, D. J.; Baker, J.; Stewart, J. P.; Head-Gordon, M.; Gonzalez, C.; Pople, J. A. Gaussian 94, Revision C.2; Gaussian, Inc., Pittsburgh, PA, 1995.
(55) Werner, H.-J.; Knowles, P. J. Molpro 96; Universität Stuttgart and University of Birmingham, 1996.

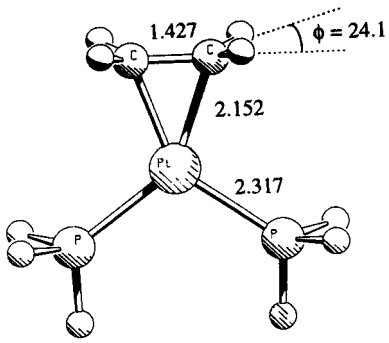

1

Figure 1. Optimized geometry of **1**, $Pt(PH_3)_2(C_2H_4)$, showing the definition of the pyramidalization angle, ϕ. Calculated values are at the B3LYP/II level.

detailed description of the method and the interpretation of the results can be found in the literature.[18,36−45]

Bond orders have been calculated using the method of Wiberg.[56] Natural bond orbital calculations[57−62] were also carried out to determine the contributions of various atomic orbitals to the Pt−P and Pt−C bonds in complex **1** and the model complexes **1a**−**f**. In these calculations the $CHOOSE keyword was used to constrain the analyses to have a total of 15 single bonds (as in structure **1**) and 4 lone pairs on platinum. This was done to ensure that platinum always had 4 bonds in these analyses, 2 to the olefin carbons and 2 to the phosphorus atoms.

Key features of the optimized geometries (including the pyramidalization angles), together with the binding energies, are presented in Table 1. The three-dimensional structures are presented in Figures 1 and 2. The results of the CDA analyses are presented in Table 2. Total energies and complete sets of Cartesian coordinates for the optimized geometries are contained in the Supporting Information.

Results and Discussion

Geometries. In Table 1 are presented experimental geometries for $Pt(PPh_3)_2(C_2H_4)$,[13,14] $Pt(PPh_3)_2(C_{11}H_{16})$,[5] $Pt(PPh_3)_2(C_{10}H_{14})$,[5] and $Pt(PPh_3)_2(C_9H_{12})$.[5] From Table 1 it can be seen that our calculated structures of **1**−**4** agree with experiment quite well (given the difference in phosphine ligands). The calculated Pt−C and Pt−P distances are systematically longer (by 0.03−0.05 Å) than the experimental values. The calculated C═C distances of **3** and **4** are only ∼0.005 Å longer than the experimental values, while the theoretical C═C bond length of **2** is 0.025 Å longer than that given by the X-ray structure analysis. The calculations predict also that **2** has a longer C═C bond than **1**, while the experimental values suggest the opposite trend (Table 1). This is difficult to understand because **2** has stronger Pt−olefin interactions than **1** (see below). It seems possible that the average C═C distance of the X-ray structure analysis of **2** does not give the correct bond length. The calculations suggest that the true C═C distance of **2** should be ∼1.44 Å. The calculated geometry of **1** agrees well with the many previous calculations that have been performed on this complex.[15,20,25−31] Frequency calculations showed that **1**, **4,** and **5** had the expected highly symmetric C_{2v} structures. In **3** there is a slight twisting of the alkene which takes it into the C_2 point group; however, this C_2 structure lies just 1.2 kJ mol^{-1} below the C_{2v} form of **3**, which is not an energy minimum structure. In **2** there is a slight twisting of the PH_3 groups which takes it into C_1 symmetry, although once again this C_1 structure lies just 0.1 kJ mol^{-1} below the C_s structure of **2**.

The geometries of **1**−**5** exhibit a clear lengthening of the C═C bond length as the degree of pyramidalization (ϕ) increases. This is accompanied by a decrease in the Pt−C distance. On the basis of these geometrical changes alone, one would predict an increase in the Pt−olefin interaction as ϕ increases. Interestingly, the change in ϕ from **2** to **3** to **4** to **5** is very similar for each step (5.4, 6.3, and 6.4°, respectively).

The calculated geometries of various fragment species are also shown in Table 1. We note in passing that our calculations for the free alkenes (n = 0−3) agree well with those of Hrovat and Borden.[34,35,63,64] For the less strained alkenes ($C_{10}H_{14}$ and $C_{11}H_{16}$), the degree of pyramidalization (ϕ) is much less than in the corresponding Pt complex. When the free alkenes are compared with the olefin ligands in the complexes, it is also apparent that the degree of C═C bond lengthening upon complexation increases as ϕ increases (from 0.096 Å in C_2H_4 to 0.133 Å in C_8H_{10}).

Finally, in Table 1 we have presented the structures of complexes **1c**−**f**, in which we have tried to model the corresponding experimental structures **2**−**5** by freezing ϕ and C−C−R at the experimental values (this follows the approach used by Morokuma and Borden previously[15]). The calculated C═C distances are in each case longer than the experimental ones, but there is a consistent overall increase from **1b** to **1f** as the pyramidalization increases. In structure **1b** we have just frozen ϕ at 0°. In structure **1a** we have frozen the complete geometry of the C_2H_4 fragment to correspond to that of free ethene.

Binding Energies. The Pt−olefin binding energies for all the complexes are shown in the last column of Table 1. The calculated value for **1** is midway in the range of theoretical values previously reported for this complex using a variety of geometries and theoretical methods: 84.9 (MP4(SDQ)),[27] 95.4 (NLSCF+QR),[30] 103 (MP2),[31] 118 (CCSD(T)),[20] and 123 kJ mol^{-1} (MP2).[15] Our calculated CCSD(T)/II value D_e = 99.9 kJ mol^{-1} is smaller than the experimental gas-phase value[65,66] for $Pt(PPh_3)_2(C_2H_4)$ of 152 kJ mol^{-1}, which could be due to three factors: (1) the treatment of electron correla-

(56) Wiberg, K. *Tetrahedron* **1968**, *24*, 1083−1096.
(57) Foster, J. P.; Weinhold, F. *J. Am. Chem. Soc.* **1980**, *102*, 7211−7218.
(58) Reed, A. E.; Weinhold, F. *J. Chem. Phys.* **1983**, *78*, 4066−4073.
(59) Reed, A. E.; Weinstock, R. B.; Weinhold, F. *J. Chem. Phys.* **1985**, *83*, 735−746.
(60) Reed, A. E.; Weinhold, F. *J. Chem. Phys.* **1985**, *83*, 1736−1740.
(61) Reed, A. E.; Curtiss, L. A.; Weinhold, F. *Chem. Rev.* **1988**, *88*, 899−926.
(62) Weinhold, F.; Carpenter, J. E. In *The Structure of Small Molecules and Ions*; Naaman, R., Vager, Z., Eds.; Plenum: New York, 1988; pp 227−236.
(63) Smith, J. M.; Hrovat, D. A.; Borden, W. T.; Allan, M.; Asmis, K. R.; Bulliard, C.; Haselbach, E.; Meier, U. C. *J. Am. Chem. Soc.* **1993**, *115*, 3816−3817.
(64) Cleven, C. D.; Hoke, S. H.; Cooks, R. G.; Hrovat, D. A.; Smith, J. M.; Lee, M.-S.; Borden, W. T. *J. Am. Chem. Soc.* **1996**, *118*, 10872−10878.
(65) Mortimer, C. T. *Rev. Inorg. Chem.* **1984**, *6*, 233−257.
(66) Martinho Simões, J. A.; Beauchamp, J. L. *Chem. Rev.* **1990**, *90*, 629−688.

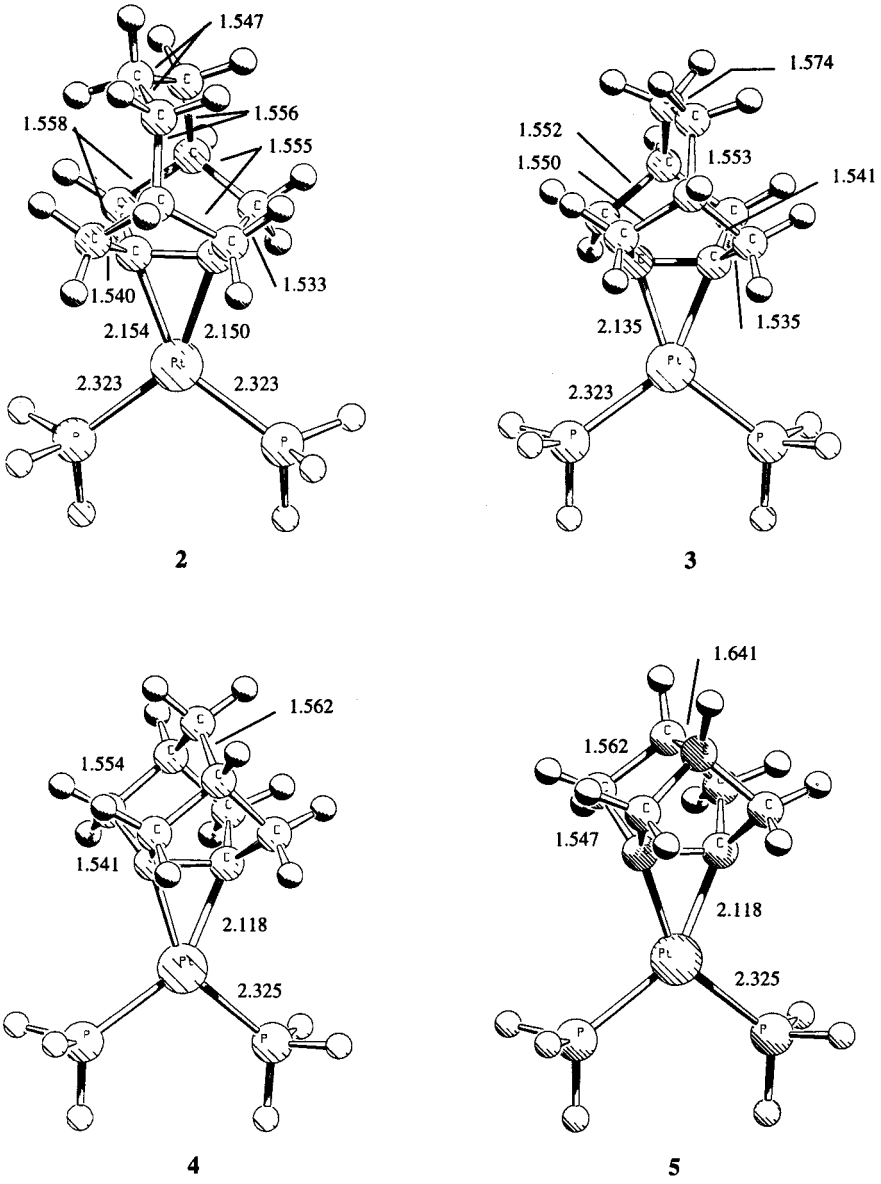

Figure 2. Optimized geometries of **2**−**5**. Bond lengths between heavy atoms are in Å at the B3LYP/II level.

Table 2. Charge Decomposition Analyses[a] and C=C Bond Orders[b] Calculated at B3LYP/II

molecule	*d*	*b*	*d*/*b*	*r*	Δ	C=C bond order
1	0.511	0.383	1.33	−0.430	−0.014	1.42
2	0.477	0.396	1.20	−0.464	−0.034	1.31
3	0.498	0.429	1.16	−0.460	−0.036	1.27
4	0.504	0.460	1.10	−0.445	−0.038	1.23
5	0.517	0.500	1.03	−0.444	−0.041	1.18
1a	0.458	0.229	2.00	−0.380	−0.005	1.61
1b	0.483	0.266	1.82	−0.406	−0.007	1.54
1c	0.517	0.448	1.15	−0.438	−0.030	1.33
1d	0.517	0.472	1.10	−0.440	−0.035	1.30
1e	0.515	0.500	1.03	−0.442	−0.041	1.27
1f	0.511	0.522	0.98	−0.443	−0.045	1.25

[a] Donation *d*, back-donation *b*, repulsive part *r*, and residual term Δ. [b] Wiberg bond index.

tion, (2) the basis set, and (3) the $PPh_3 \rightarrow PH_3$ approximation.

The first of these factors can be ruled out, since we have used CCSD(T), which is generally regarded as one of the best treatments of (nondynamical) electron correlation currently available. Previous calculations have shown that metal−ligand bond energies which are calculated at CCSD(T)/II without BSSE corrections are in very good agreement with experimental values.[20,37,67,68] The second and third factors require careful thought and evaluation. We have completed preliminary calculations on $Pt(PMe_3)_2(C_2H_4)$ and $Pt(PPh_3)_2(C_2H_4)$ at the B3LYP/II level of theory and find that the binding energies are calculated to be 49.1 and 69.7 kJ mol^{-1}, respectively. At the same level of theory, the binding energy of **1** is calculated to be 64.4 kJ mol^{-1}, which suggests that the $PPh_3 \rightarrow PH_3$ approximation may not be the problem. We are currently carrying out further calculations on the binding energy of $Pt(PR_3)_2(C_2H_4)$ with different R groups and improved basis sets, and this work will be published in a detailed separate paper, together with results obtained from QM/MM methods.

The effect of including ZPVE corrections for **1**−**5** is to lower the calculated binding energies of all the complexes by several kJ mol^{-1}. For **1** we have calculated

(67) Ehlers, A. W.; Frenking, G. *J. Chem. Soc., Chem. Commun.* **1993**, 1709−1711.
(68) Ehlers, A. W.; Frenking, G. *J. Am. Chem. Soc.* **1994**, *116*, 1514−1520.

the B3LYP/II, MP2/II, and CCSD(T)/II D_e binding energies (64.4, 140.7, and 99.9 kJ mol^{-1}, respectively). Interestingly, the B3LYP value is too low and the MP2 value is too high by about the same amount, so that the CCSD(T) value is almost the average of the B3LYP and MP2 values. Size limitations prevented us from carrying out CCSD(T) calculations on complexes **2**−**5**, and so for these systems we have used the isostructural reaction approach[53] to obtain approximate CCSD(T)/II values for the binding energies. This approach has been shown to give reliable estimates for a series of similar molecules.

The binding energies increase strongly as one moves from the ethene complex **1** to complexes with progressively more strained olefins: **2** < **3** < **4** < **5**. Interestingly, across this series the binding energy increases almost linearly by 50 kJ mol^{-1} for each structure. The binding energy of **5** is nearly twice that of **2**. The increase in binding energy may be correlated with the increase in pyramidalization angle, ϕ, although clearly other geometrical changes are involved as well.

Finally, in Table 1 we have presented the binding energies for the model complexes **1a**−**f**. Following a suggestion of Morokuma and Borden,[15] in calculating the binding energies of **1c**−**f** we have frozen the pyramidalization and C−C−H angles in the model complexes at the values in the corresponding experimental structures, and in addition we have frozen the pyramidalization and C−C−H angles in the free ethenes to correspond to the calculated structures of the tricyclic alkenes. The binding energies of **1c**−**f** roughly parallel those of **2**−**5**, although there is a clear divergence as the magnitude of the binding energy increases. On this basis, it appears that complex **1f** is probably a poor model for complex **5** in that it underestimates the various factors involved in the high binding energy of **5**.

A comparison of **1** with **1a** shows that the undistorted ethene fragment, via donation/back-donation, gives 50% of the binding energy of **1**. The other 50% comes from the better interaction of the distorted olefin. By comparing **1b** with **1a**, we can conclude that 10% comes from allowing the C═C bond to stretch in the complex and the other 40% from allowing the ethene to "bend". The energy difference between ethene in its equilibrium geometry and in a frozen geometry corresponding to complex **1** is 48.0 kJ mol^{-1}. Thus, the gain in binding to the metal fragment afforded by distorting the alkene significantly outweighs this penalty.

Charge Decomposition Analyses. The results for the charge decomposition analyses (CDA) are displayed in Table 2. For all the complexes, the residual term (Δ) is very small, which indicates that it is appropriate to consider these structures as donor−acceptor complexes and to interpret their bonding in terms of the Dewar−Chatt−Duncanson model.

The CDA results for **1** suggest that the donor−acceptor interactions on the olefin side do not involve only the HOMO and LUMO of ethene, i.e., the π and π^* orbitals. There are four molecular orbitals of the complex which, according to the CDA results, contribute about the same extent to the olefin→Pt donation. Three of them involve dominantly C═C π-bonding character on the olefin side, as expected. The fourth is interesting

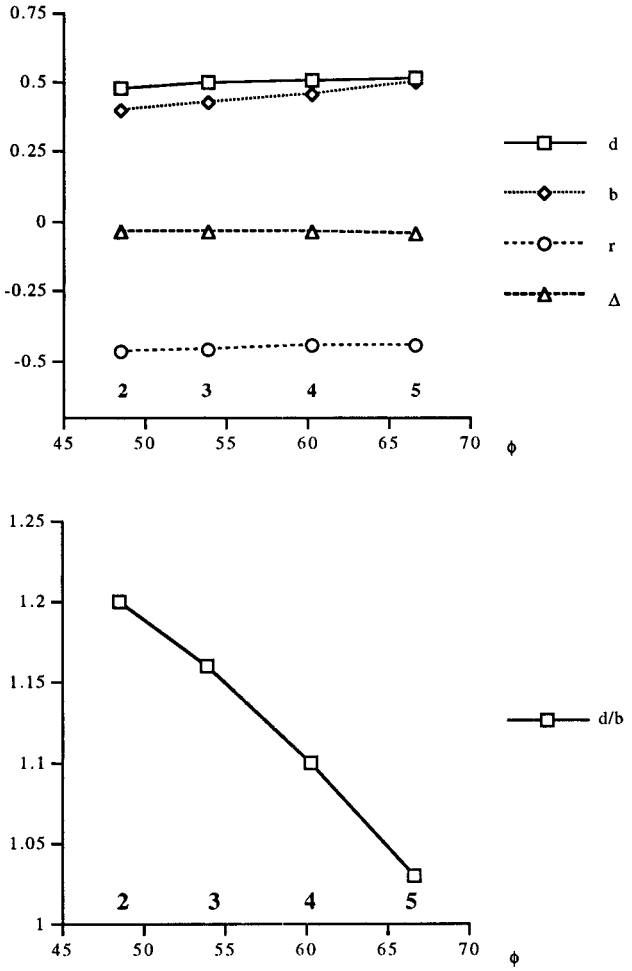

Figure 3. CDA values plotted against pyramidalization angle (degrees) for complexes **2**−**5**.

in that it is the lowest in energy of the valence molecular orbitals of the complex, which corresponds on the olefin side to the C−C σ bond formed from the 2s orbitals on the carbons. All four of these molecular orbitals are of a_1 symmetry and involve donation to the $d_{x^2-y^2}$ and d_{z^2} orbitals of platinum. Only one molecular orbital is implicated in the olefin←Pt back-donation. It is of b_2 symmetry and involves the d_{xz} orbital on platinum and the π^* orbital on the carbons (together with a contribution from the p_x and p_z orbitals on phosphorus, as expected[23,24]). Finally, the repulsive polarization part of the CDA shows contributions from all five of the molecular orbitals discussed above and confirms that all five are equally responsible for the binding of ethene and platinum in **1**.

Although a number of orbitals are involved in the interactions in **1**, as one moves to the larger complexes **2**−**5** life gets easier (perhaps counterintuitively). A single molecular orbital dominates each of the donation and back-donation interactions. In each case, the dominant orbital in the olefin→Pt donation interaction involves the C═C π system and the s, d_{z^2}, and $d_{x^2-y^2}$ orbitals on platinum. The dominant orbital in each of the olefin←Pt back-donation interactions involves the platinum d_{xz} orbital and the C═C π^* system.

The CDA values for **2**−**5** are plotted against the pyramidalization angle in Figure 3. This clearly shows that *b* increases faster than *d* as ϕ increases. More

importantly, however, complexes **1**−**5** also show a steady decrease in the *d*/*b* ratio. This indicates beautifully the increasing importance of the olefin←Pt back-donation as the olefin becomes more pyramidal. It follows that lowering the energy level of the LUMO of the olefin is more important than raising the energy level of the HOMO to achieve stronger metal−olefin interactions. This is an important result which is helpful for the experimental design of new metal−olefin complexes. Since a pyramidalization of the olefin might be expected to yield a higher lying HOMO and lower lying LUMO (the DFT calculations, however, do not show a rise of the HOMO (see below), in agreement with previous computational[34] and experimental[63] findings), it is not easy to decide *a priori* which of the two factors is more important for the increase in the bond strength. Indeed, the CDA results for the different contributions show that the olefin→Pt donation *and* the olefin←Pt back-donation increase with **2** < **3** < **4** < **5** (Table 2). The calculated *d*/*b* ratio shows that the increase of the back-donation is larger. The conclusion made from the CDA results, that the LUMO is more important, is in agreement with the previous work of Ziegler[23] and others,[2,21,69] who showed that the olefin←metal back-donation is more important for the metal−ligand bonding than olefin→metal donation. The CDA results are also in agreement with the conclusions based on the measured NMR chemical shifts and coupling constants of the complexes **2**−**4** of Borden and co-workers.[5] Previous theoretical analyses using extended Hückel theory (EHT) calculations have also demonstrated the importance of the HOMO of the metal fragment in the Pt−olefin binding interaction;[70] however, this effect has not been studied directly in the present work.

Despite the fact that the HOMO energies of the free olefins show little change with increased pyramidalization (see below), donation in the complexes increases with increased pyramidalization. In explaining this apparent paradox, Nicolaides *et al*.[5] argued that, since back-donation transfers charge into the olefin LUMO, the resulting Coulomb repulsion makes the HOMO a better donor in the complexes as pyramidalization, and hence back-donation, increases. The present CDA results provide strong support for this interpretation.

The changes in the *d*/*b* ratio from **1** to **5** are accompanied by a decrease in the C═C bond order, confirming that there is less of a carbon−carbon double bond in the more strained olefin complexes, as might be expected.

The CDA results for the model complexes **1a**−**f** are also shown in Table 2. Olefin→Pt donation is significantly larger than olefin←Pt back-donation in the complexes with planar ethylene **1a** and **1b**, but back-donation rises significantly (lower *d*/*b* ratio) when the ethylene ligand becomes more pyramidal. Once again the C═C bond order of **1a**−**f** decreases steadily, which is consistent with the increase in binding energy in Table 1 and therefore an increase in the Pt−olefin interaction. The CDA results for **1c**−**f** show much less variation in the *d*, *b*, and *r* values compared to the case for **2**−**5**, but the trend in the *d*/*b* ratio in the model complexes is very similar to that in the larger systems.

Table 3. Natural Bond Orbital Analyses Calculated at B3LYP/II

molecule	ϕ^a	Pt−P[b] 6s (Pt)	Pt−C[b] 6s (Pt)	Pt−C[b] 2s (C)
1a	0.0	0.61	0.21	0.15
1b	0.0	0.61	0.24	0.17
1	24.1	0.59	0.30	0.30
1c	48.3	0.57	0.39	0.35
1d	55.1	0.56	0.40	0.38
1e	62.3	0.55	0.41	0.42
1f	66.6	0.55	0.42	0.46

[a] Pyramidalization angle. [b] Presented in these columns are the absolute values of the coefficients of the 6s (platinum) and 2s (carbon) natural atomic orbitals in the Pt−P and Pt−C natural bond orbitals.

Table 4. HOMO and LUMO Energies[a] and Olefin Strain Energies[b] for the Free Alkenes in Systems 1−5

alkene	HOMO (π)	LUMO (π^*)	OSE
C_2H_4	−7.25	0.51	0
$C_{12}H_{16}$	−5.56	0.44	74.1
$C_{10}H_{14}$	−5.49	−0.05	156
C_9H_{12}	−5.42	−0.63	219
C_8H_{10}	−5.58	−1.40	305

[a] In eV, calculated at B3LYP/II. [b] In kJ mol^{-1}, from ref 34.

NBO Analyses. The results of the natural bond orbital (NBO) analyses are shown in Table 3. It can be seen that as the pyramidalization angle increases there is a decrease in the platinum 6s character in the Pt−P bond orbital and an increase in the 6s character in the Pt−C bond orbital. At the same time there is an increase in the contribution from the 2s atomic orbitals on carbon to the Pt−C bond orbital. These results are beautifully consistent with the conclusions drawn from NMR studies of the ^{31}P−^{195}Pt and ^{13}C−^{195}Pt coupling constants of complexes **2**−**4** by Borden and co-workers.[5] Our analyses of the remaining dominant contributions to the natural bond orbitals for Pt−C show that there are slight changes in the contributions from $2p_y$ and $2p_z$ on carbon as the pyramidalization angle increases (this corresponds to a reorientation of the π bond, as expected), while for the Pt−P bond orbitals the contributions from the dominant atomic orbitals on phosphorus, 3s, $3p_y$, and $3p_z$, do not change at all. The changes in the contributions of the 5d and 6p atomic orbitals on platinum are hard to disentangle but appear to be small.

Predictions. The binding energies for **1**−**5** are plotted against a range of measures in Figure 4. The extra data used to generate the plots are summarized in Table 4. The olefin strain energy (OSE) has been calculated for the tricyclic olefins with $n = 0-3$ by Borden[34] and is defined as the extra strain introduced into the system by the double bond.[71] Good correlation in the energy plots for **2**−**5** is seen for D_e vs *b*, D_e vs π^*, D_e vs $\phi_{complex}$, and D_e vs OSE (perhaps the best), and the correlation is only slightly less good for D_e vs *d*, D_e vs *d*/*b*, and D_e vs $\phi_{free\ alkene}$. D_e vs π is relatively constant for **2**−**5**. Simple empirical relationships between the binding energies of metal−olefin complexes and various HOMO−LUMO energies have been discussed previously.[5,34,63,72]

(69) Nelson, J. H.; Jonassen, H. B. *Coord. Chem. Rev.* **1971**, *6*, 27−63.
(70) Hofmann, P.; Heiss, H.; Müller, G. *Z. Naturforsch.* **1987**, *42B*, 395−409.
(71) Maier, W. F.; Schleyer, P. v. R. *J. Am. Chem. Soc.* **1981**, *103*, 1891−1900.
(72) Tolman, C. A. *J. Am. Chem. Soc.* **1974**, *96*, 2780−2789.

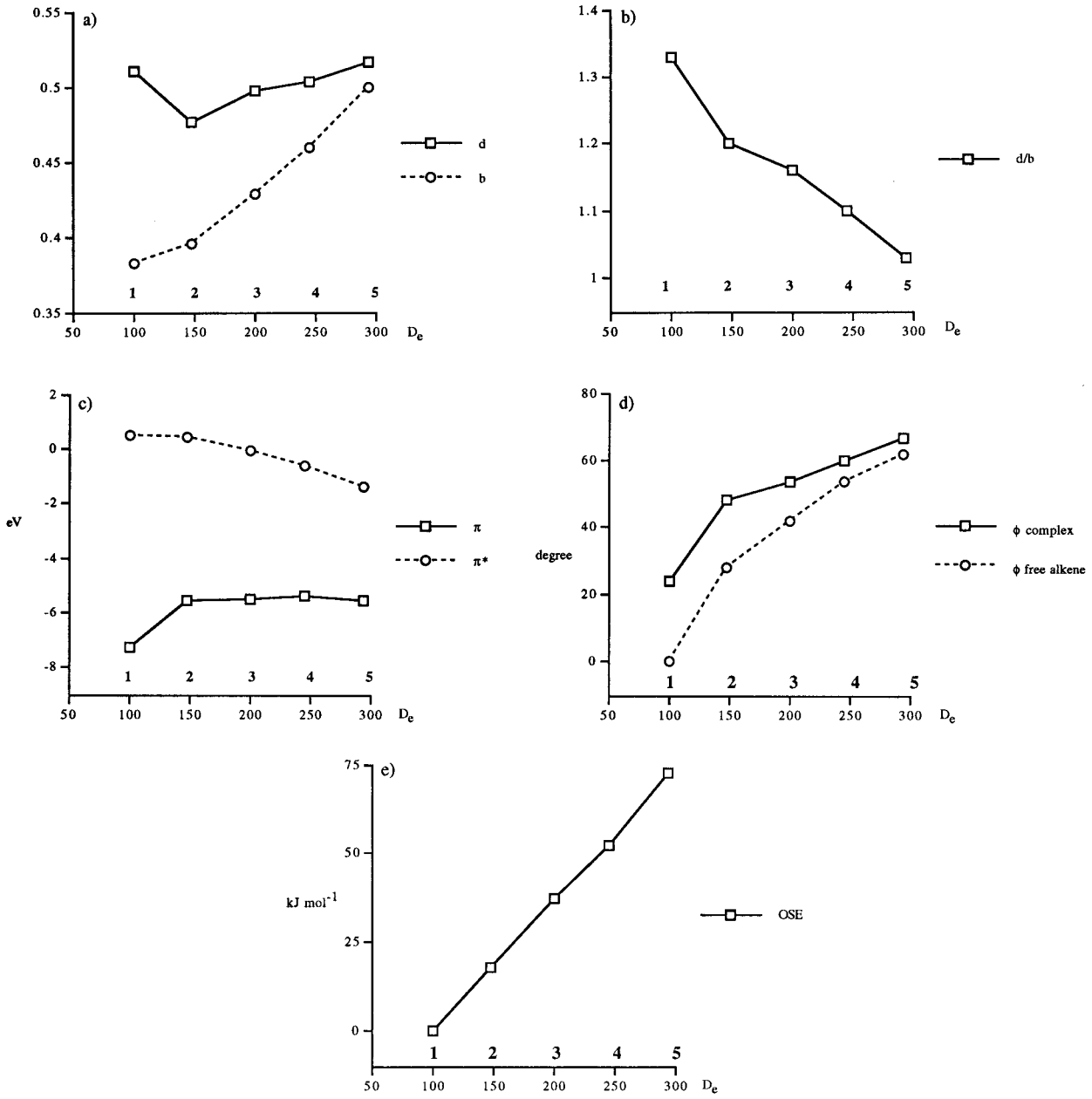

Figure 4. Binding energies (kJ mol^{-1}) of complexes **1**−**5** plotted against (a) *d* and *b*, (b) *d*/*b*, (c) π and π^* energy of olefin, (d) the pyramidalization angles in the complex and in the free alkene, and (e) olefin strain energy.

For most of the correlations in Figure 4 there is a kink in the graph on going from **1** to **2**. However, the good correlation with π^* and OSE encompasses C_2H_4 as well as the tricyclic alkenes. Overall, the olefin strain energy appears to give the best correlation with binding energy (Figure 4e).

We have also plotted the back-donation values, *b*, in Table 2 against the strain energies and pyramidalization angles for **1**−**5** in Figure 5. This shows a good correlation and indicates that the amount of back-donation interaction in the complex may be fairly well predicted by the OSE of the free alkene.

From the discussion above, it appears that as a rough rule of thumb the π^* energy or the OSE of the free alkene would be a good predictor of the Pt−olefin binding energy for a series of related olefins, where the Pt part of the complex is kept constant. Can we use this knowledge to predict the binding energies of other strained olefins? OSE's have been calculated for **6** (cubene, 246 kJ mol^{-1}),[34] **7** (279 kJ mol^{-1}),[34] and **8** (about the same value as for the $n = 2$ $C_{10}H_{14}$ alkene in the present study).[71] From Figure 4e, one could predict

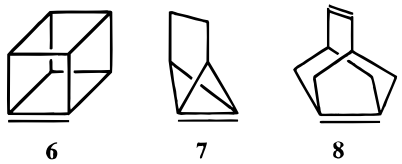

6 **7** **8**

that the binding energies of these olefins with $Pt(PH_3)_2$ would be about 250, 275, and 200 kJ mol^{-1} for **6**, **7**, and **8**, respectively. It would be interesting to test these predictions with further calculations. It would also be interesting to calculate OSEs for other series of pyramidalized olefins and for the substituted cyclopropenes

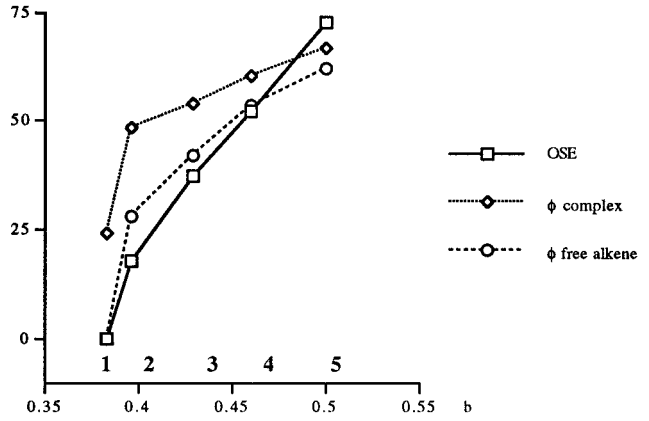

Figure 5. Values of *b* for complexes **1**−**5** plotted against olefin strain energy (kJ mol^{-1}) and the pyramidalization angles (degrees) in the complex and in the free alkene.

and again make predictions about the likely Pt−olefin binding energies.

Finally, could one extend these predictions to other metal systems (eg Pd or Ni)? From the work of Tolman[72] we would expect there to be similar correlations for Ni(0)− and Fe(0)−olefin complexes. In the present study, we have not analyzed the orbital energies of the metal fragments prior to complexation. Such an analysis will be the topic of a future work.

Summary

The binding energies for a series of Pt−tricyclic olefin complexes have been calculated for the first time. As expected, the binding energies increase as the strain in the olefin increases. The "charge decomposition analysis" procedure is shown to be a powerful quantitative tool for understanding the bonding in these complexes, and all the systems discussed here fit the classical olefin→Pt donation and olefin←Pt back-donation picture of Pt−olefin binding. Natural bond orbital analyses are in agreement with the conclusions derived from previous NMR experiments. The π^* molecular orbital energy and the olefin strain energy of the free olefin appear to be good qualitative predictors of the likely strength of the Pt−olefin interaction and may be used to design strongly bound complexes.

Acknowledgment. We thank Prof. Weston Thatcher Borden for valuable discussions. The Australian Academy of Science is gratefully acknowledged for providing funding to B.F.Y. for a 1-month visit to Marburg, during which much of this work was carried out. This work was also supported by the Fonds der Chemischen Industrie, the Deutsche Forschungsgemeinschaft, and the Australian Research Council. B.F.Y. is also grateful to Stefan Fau and Nikolaus Fröhlich for patiently answering many questions.

Supporting Information Available: A complete listing of B3LYP/II optimized geometrical coordinates for structures **1**−**5** and the fragment species, together with listings of total energies, zero-point vibrational energies, $\nu_{C=C}$ vibrational frequencies, and single-point total energies at the MP2/II and CCSD(T)/II levels. This material is available free of charge via the Internet at http://pubs.acs.org.

OM9805842